Supplementary Information

for

Controlled Scalable Synthesis of Uniform, High-Quality Monolayer and Few-layer MoS_2 Films

Yifei Yu[1], Chun Li[1], Yi Liu[3], Liqin Su[4], Yong Zhang[4], Linyou Cao[1,2]*

[1]Department of Materials Science and Engineering, North Carolina State University, Raleigh NC 27695; [2]Department of Physics, North Carolina State University, Raleigh NC 27695; [3]Analytical Instrumentation Facility, North Carolina State University, Raleigh NC 27695; [4]Department of Electrical and Computer Engineering, The University of North Carolina at Charlotte, Charlotte, NC 28223

* To whom correspondence should be addressed.
Email: lcao2@ncsu.edu

This PDF file includes:

Figs. S1- S11

Figs. S12-S16

Studies of the growth mechanism with Figs. 17-25

References

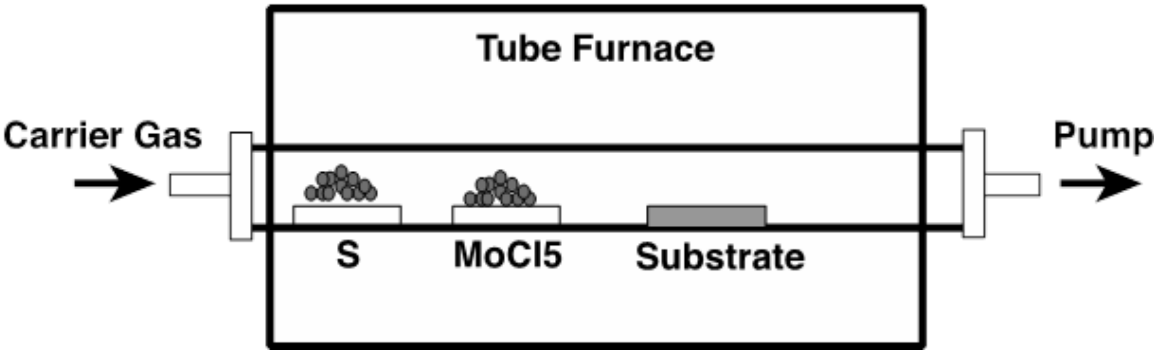

Fig. S1 Schematic illustration of the synthetic setup used for the non-catalytic chemical vapor deposition growth of atomic-thin MoS_2 films.

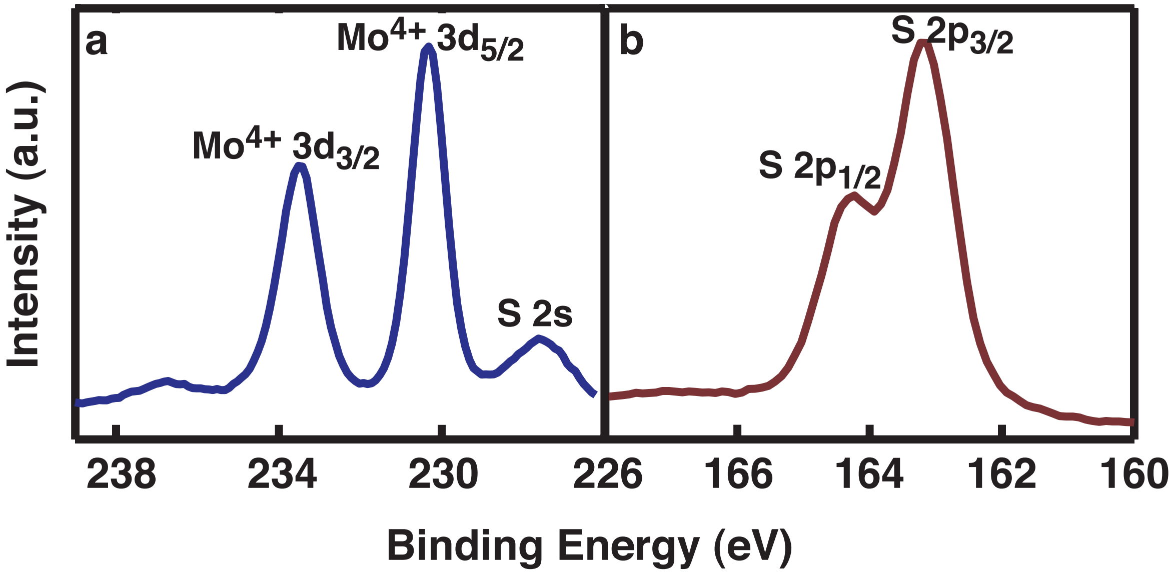

Fig. S2 X-ray photoemission spectroscopy of synthetic MoS_2 films. Binding energies for (a) Mo atoms and (b) sulfur atoms.

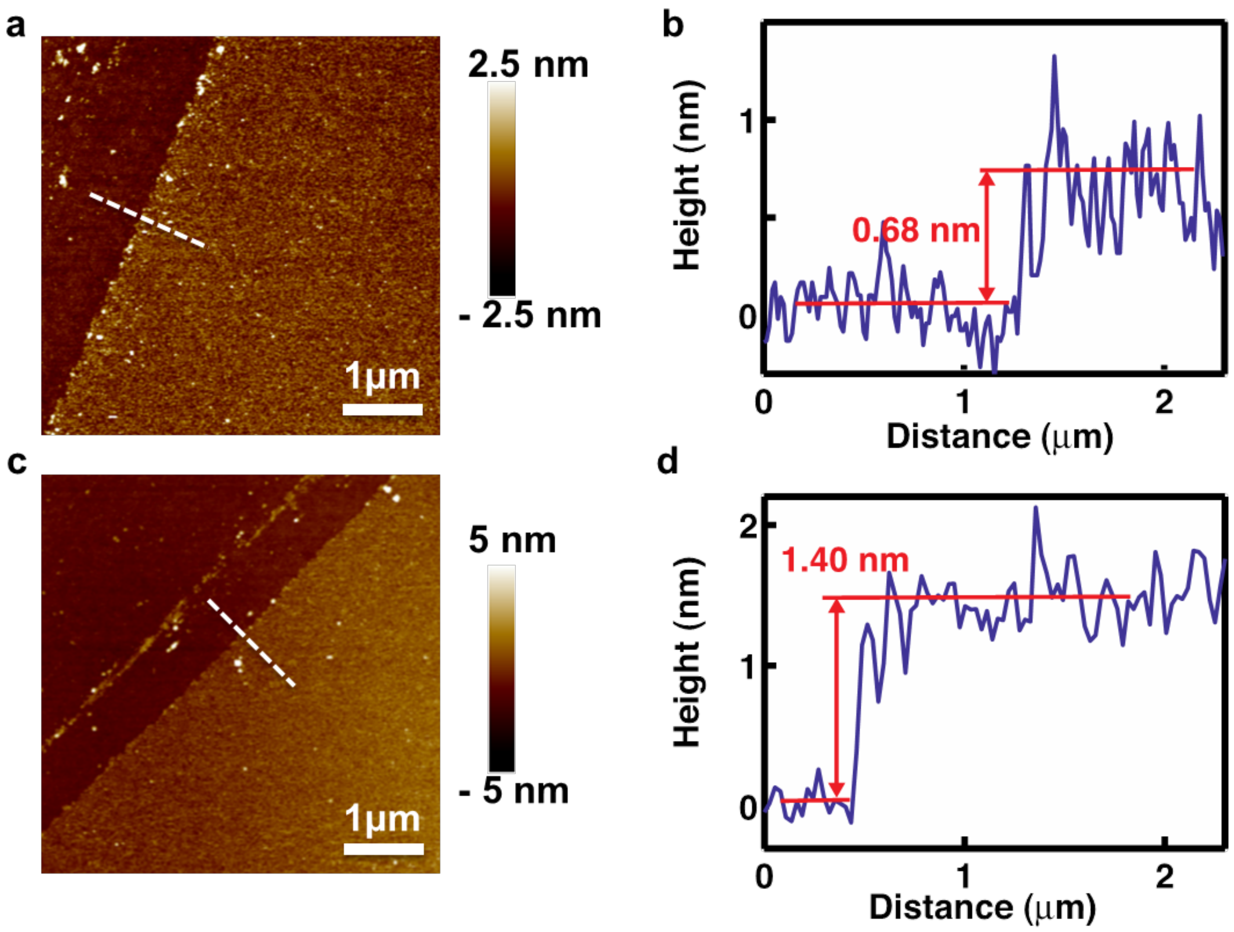

Fig. S3 AFM characterization of the MoS_2 monolayer and bilayer films grown on sapphire substrates. (a) Typical AFM image of the synthetic monolayer. The area occupied by the MoS_2 is labeled as shown. (b) Height profile for the white dashed line shown in (a). (c) Typical AFM image of the synthetic bilayer. The area occupied by the MoS2 is labeled as shown. (d) Height profile for the white dashed line shown in (c).

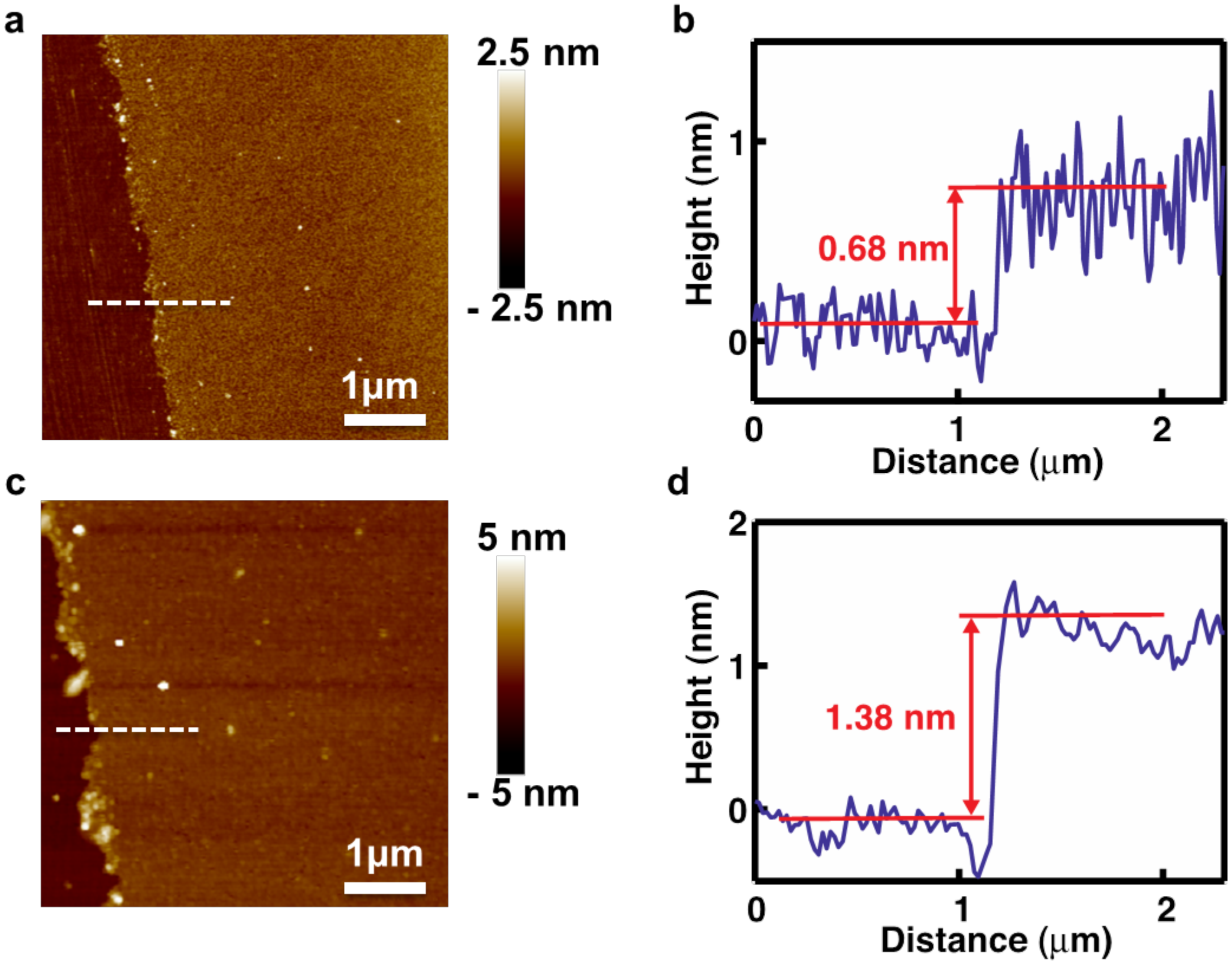

Fig. S4 AFM characterization of the MoS_2 monolayer and bilayer films grown on SiO_2/Si substrates. (a) Typical AFM image of the synthetic monolayer. The substrate and the MoS_2 thin film are labeled as shown. (b) Height profile for the white dashed line shown in (a). (c) Typical AFM image of the synthetic bilayer. The substrate and the MoS_2 thin film are labeled as shown. (d) Height profile for the white dashed line shown in (c).

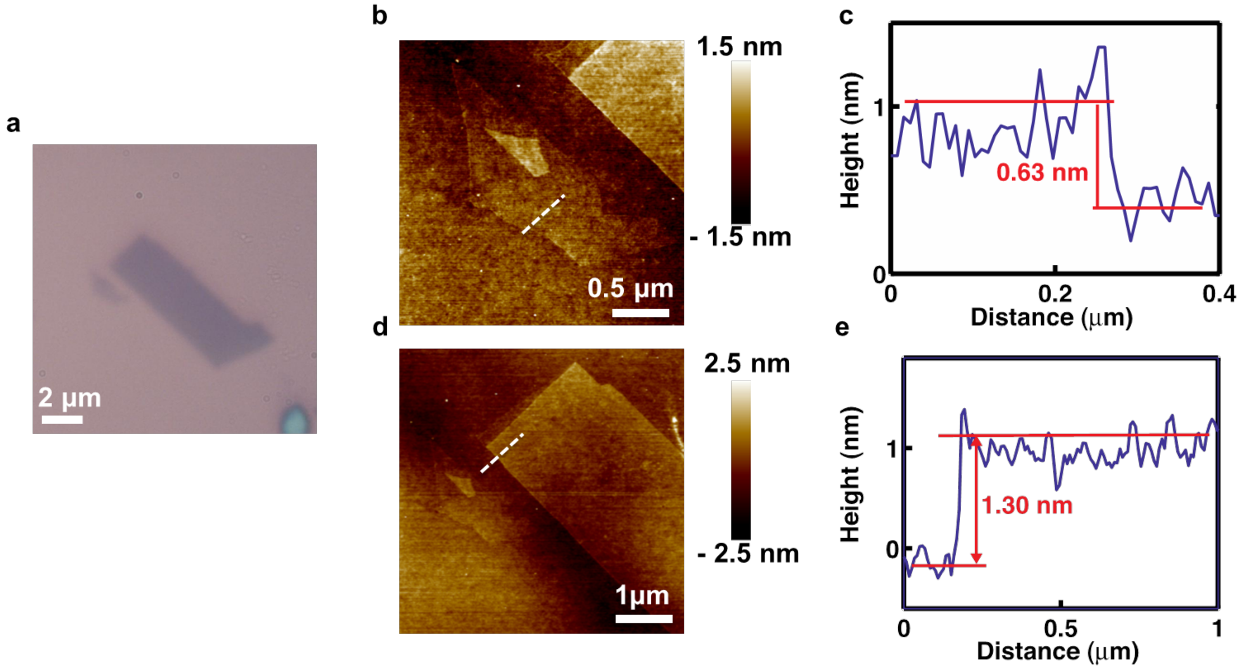

Fig. S5 Characterization of exfoliated MoS_2 monolayer and bilayer. (a) Optical image of exfoliated monolayer and bilayer dispersed on SiO_2/Si substrates. (b and d) AFM images of the exfoliated MoS_2 monolayer and bilayer. The two images have different magnification to better illustrate the monolayer and the bilayer, respectively. (c and e) Height profile for the white dashed shown in (b) and (d).

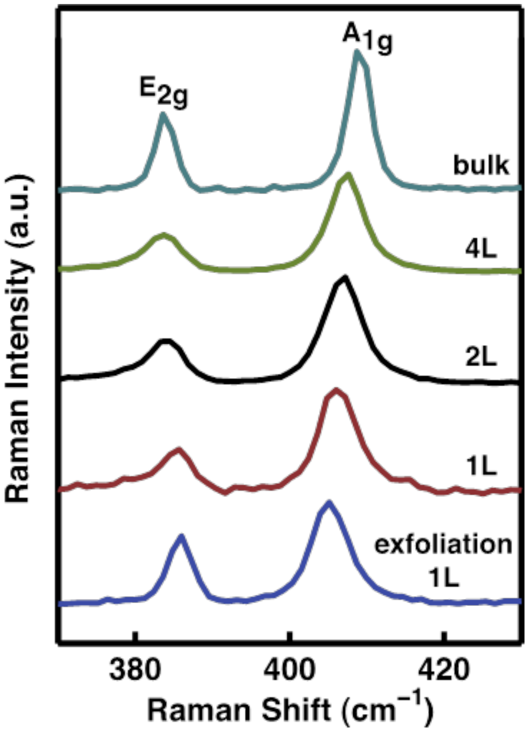

Fig. S6 Raman spectra of the MoS_2 monolayer (1L), bilayer (2L), and tetralayer (4L) films grown on SiO_2/Si substrates. Also given are the Raman spectra of exfoliated MoS_2 monolayer and bulk MoS2 dispersed on SiO_2/Si substrates. The two characteristic Raman modes are labeled.

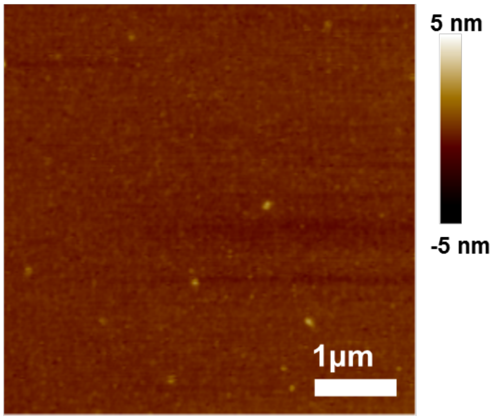

Fig. S7. Topview of the AFM image given in Figure 2D of the text, roughness < 0.2 nm.

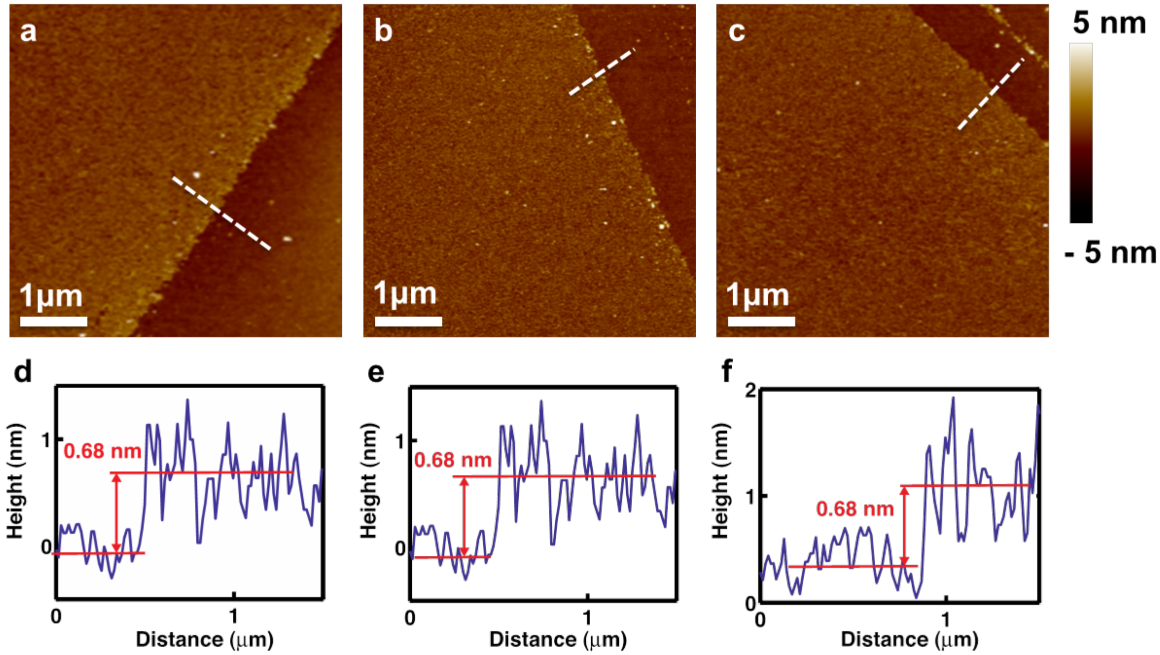

Fig. S8 (a, b, and c) AFM images taken from different area of a MoS_2 monolayer grown on sapphire. The distances between the positions that the images were collected from are at least 1 cm. (d, e, and f) Height profiles for the white dashed lines given in (a), (b), and (c), respectively.

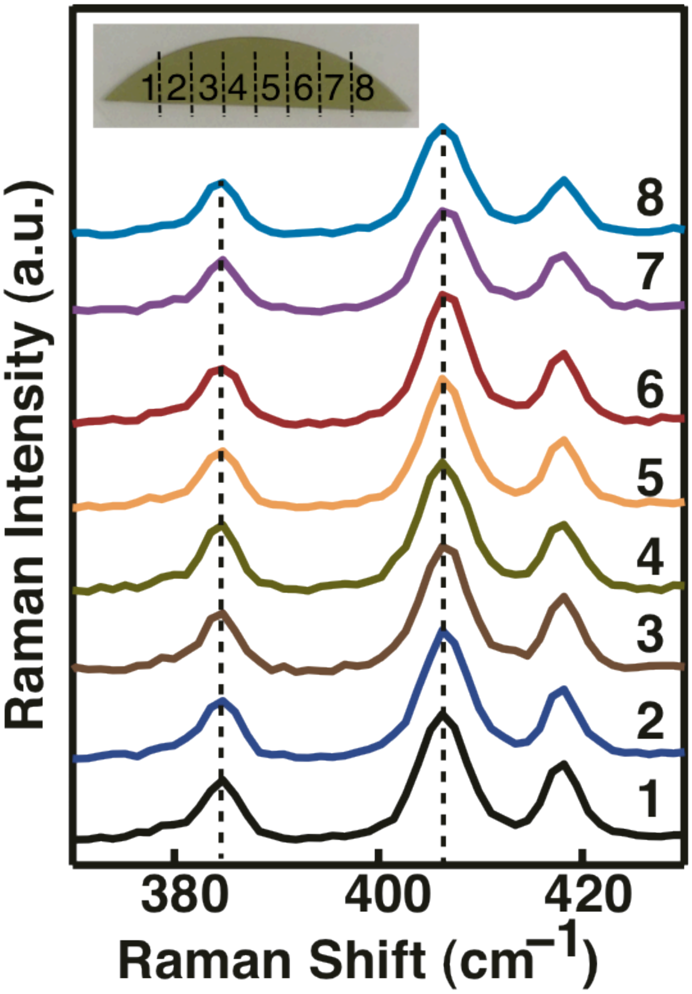

Fig.S9 Raman spectra collected from eight different areas of the MoS_2 bilayer film grown on sapphire. The inset shows the eight areas evenly distributes across the substrate.

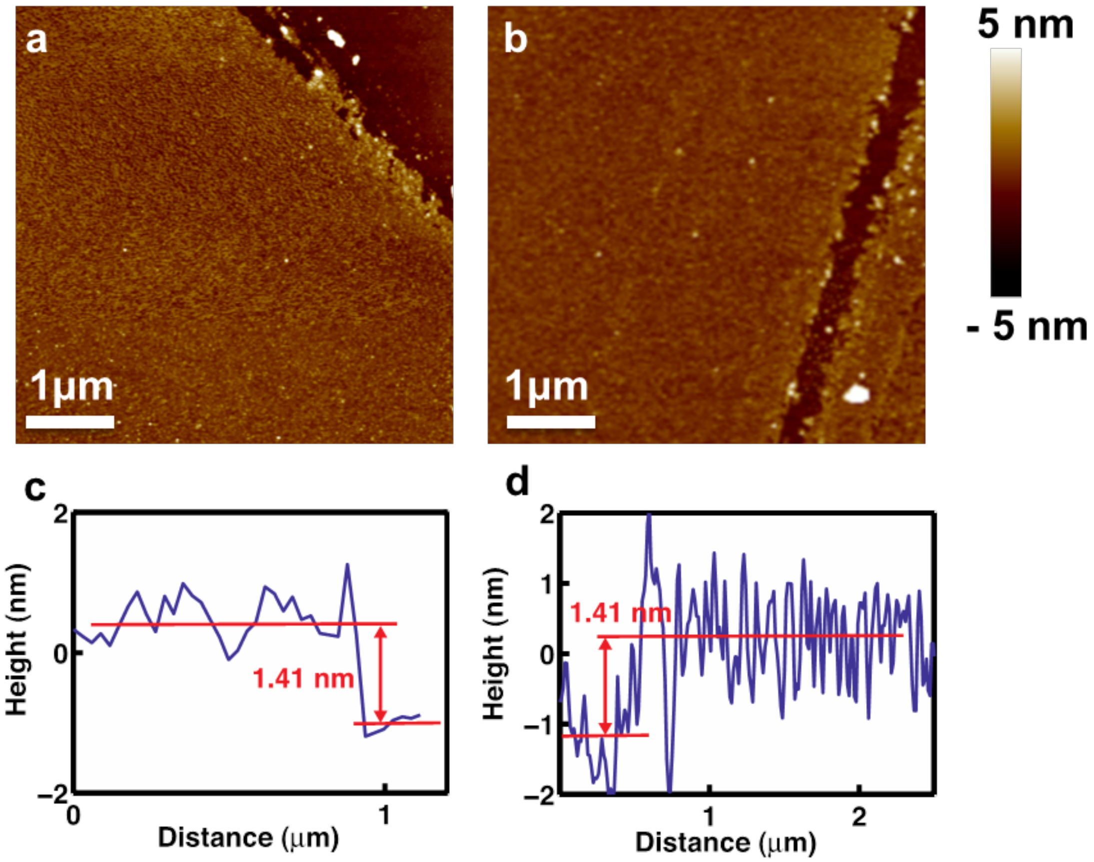

Fig. S10. (a and b) AFM images collected from different areas of a MoS_2 bilayer grown on sapphire. The distance between the positions that the images were collected from is larger than 1 cm. (c and d) Height profiles for the white dashed lines given in (a) and (b), respectively.

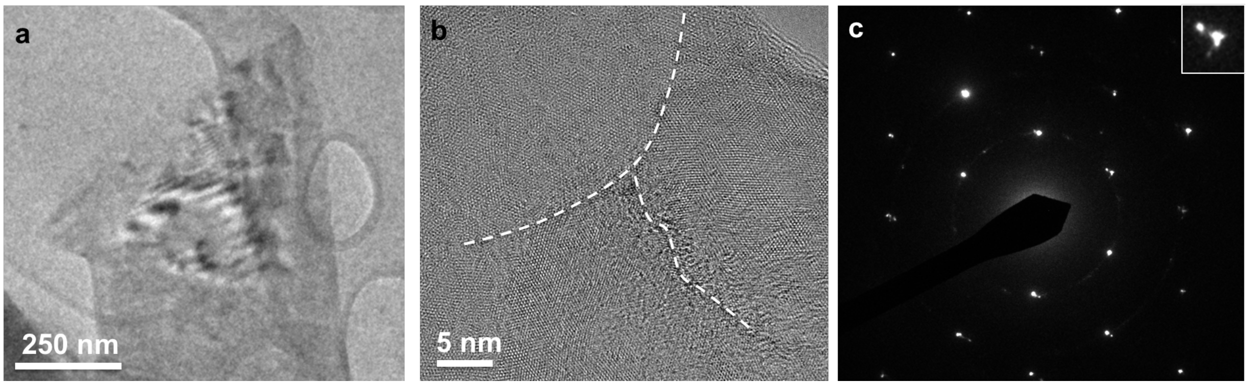

Fig. S11 Transmission electron microscope characterization of synthetic MoS_2 films. (a) Typical TEM image of synthetic MoS2 films. (b) TEM image showing multiple crystalline domains. The white dashed lines indicate the domain boundary. (c) Typical selected area electron diffraction for the synthetic MoS_2 film. Inset, a magnified diffraction spot showing multiple points involved. This indicates the synthetic thin film is polycrystalline.

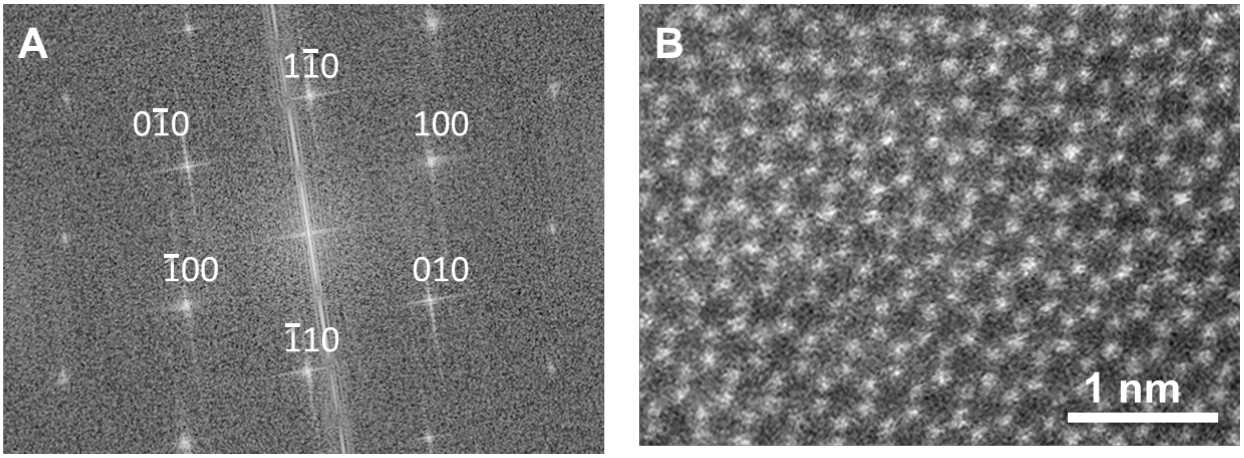

Fig. S12. (a) FFT pattern of the atomic image shown in Figure 3a of the text. The pattern is indexed. (b) The original HAADF image of Figure 3c in the text.

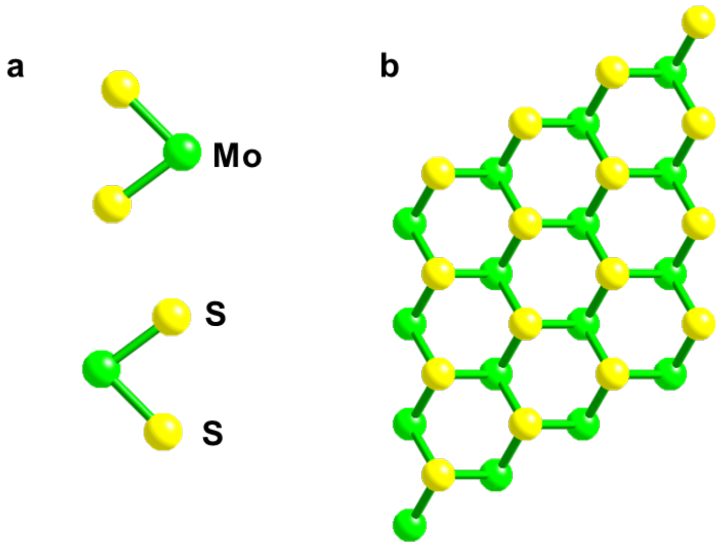

Fig. S13 Structure model for 2H-MoS2. (a) Crystal structure viewed from [010] direction. (b) Crystal structure viewed from [001] direction. The green dot indicates the Mo atom, and the yellow the S atom.

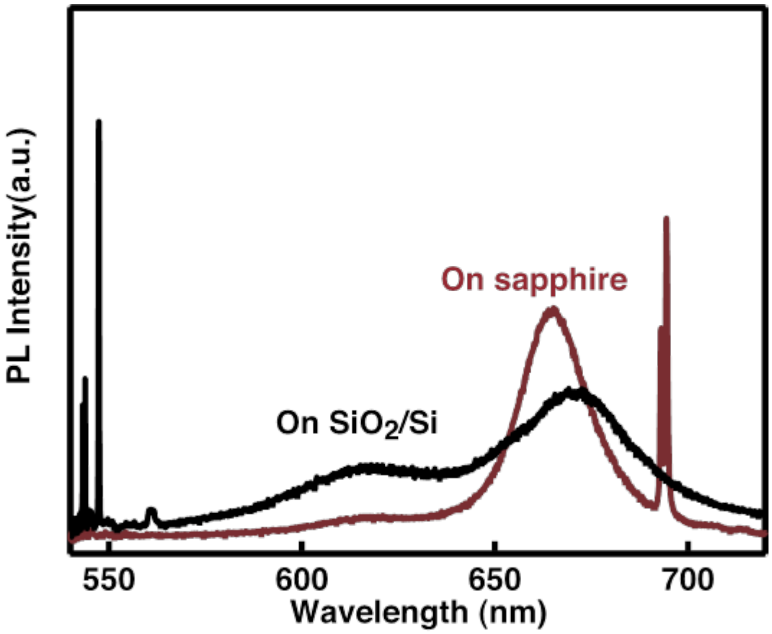

Fig. S14 Photoluminescence of an as-grown MoS_2 monolayer on sapphire (red) and of the same monolayer transferred to SiO_2/Si substrate.

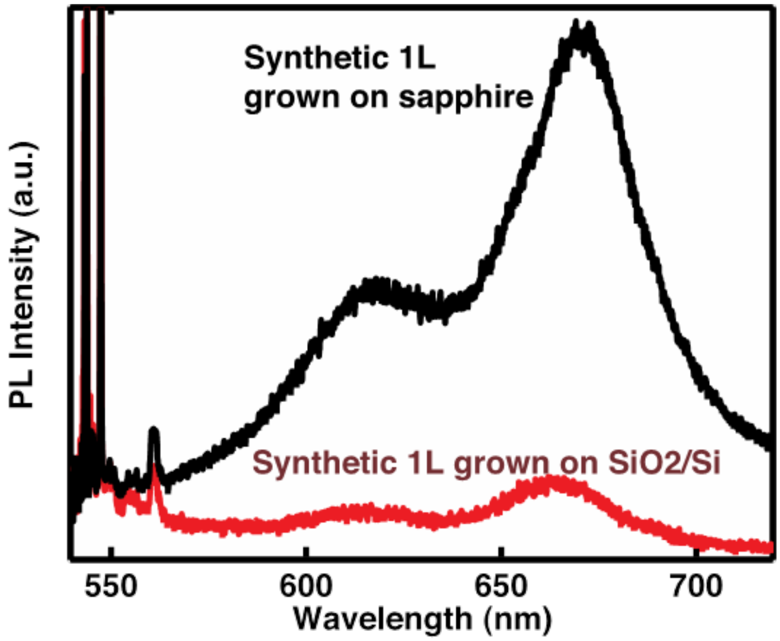

Fig. S15 Photoluminescence of synthetic MoS_2 grown on sapphire (black) and on SiO_2/Si (red). The monolayer grown on sapphire was transferred to SiO_2/Si substrates for the PL measurement.

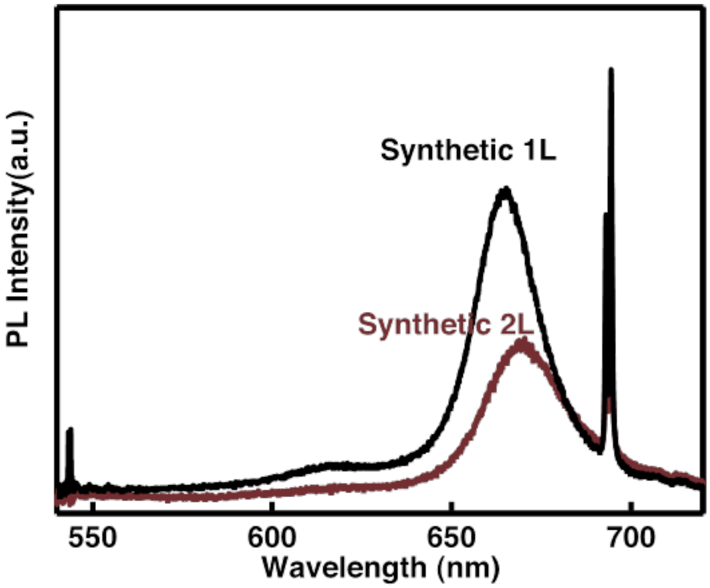

Fig. S16 Photoluminescence of an as-grown MoS_2 monolayer (black) and bilayer (red) on sapphire (red).

Studies of the Growth Mechanism

We found that the layer number of resulting MoS_2 thin films shown dependence on the amount of $MoCl_5$ used in experiments. A larger amount of $MoCl_5$ generally yields thicker films. With typical experimental conditions, using 1-4 mg $MoCl_5$ gives rise to MoS_2 monolayers, 5-10 15 mg for MoS_2 bilayers, 15- 25 mg for MoS_2 trilayers, and 25-35 mg for quadra-layers (Fig. S17-S18). We cannot see substantial deposition of MoS_2 when the amount of $MoCl_5$ is decreased down to less than 1 mg. And the precise control of the layer number tends to be more difficult for thicker films. Table 1 lists the correlation between the amount of $MoCl_5$ used in experiments and the lay number of resulting MoS_2 thin films. Also listed is the frequency difference Δk between the A_{1g} and E_{2g} peaks in the Raman spectra of these thin films.

Table S1. Correlation of the amount of $MoCl_5$ vs. the layer number of MoS_2 films*

Amount of $MoCl_5$	< 1mg	1- 4 mg	5- 15 mg	15-25 mg	25- 35 mg
Layer number of MoS_2 film	No deposition	1 layer	2 layer	3 layer	4 layer
Δk (A_{1g}-E_{2g})	N/A	20.2 - 21.2 cm^{-1}	22.4 -23.2 cm^{-1}	23.6 -23.9 cm^{-1}	24.0 - 24.2 cm^{-1}

* Note: The typical experimental conditions used in these growths include: temperature, 850°C; total pressure, 2-3 Torr; flow rate, 50 sccm Ar; amount of sulfur, 1 g. To achieve a uniform growth, the substrates were typically placed 1-7 cm away from the center of the furnace.

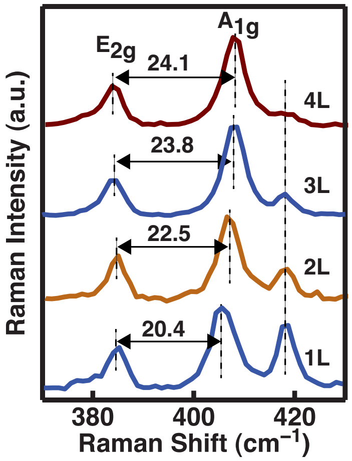

Fig. S17. Raman spectra of the MoS_2 thin films grown using different amount of $MoCl_5$. These thin films have different layer numbers (1L, 2L, 3L, and 4L) as labeled. The layer number was confirmed by AFM as shown in Fig. S18. The dashed line to the right indicates the Raman peak of the sapphire substrate. The other two dashed lines indicate the positions of the E_{2g} and A_{1g} peaks of MoS_2 thin films. The frequency difference between the two peaks is given in the figure.

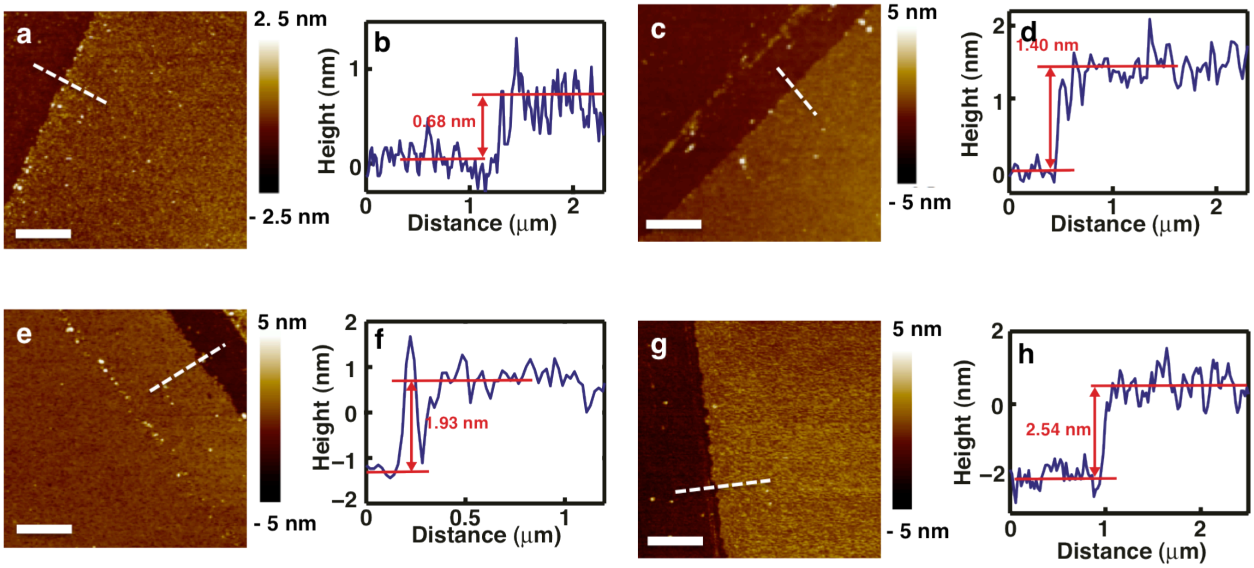

Fig. S18. AFM measurements of the MoS_2 thin films grown using different amount of $MoCl_5$. (a, c, e, g) AFM images of MoS_2 thin films; (b, d, f, h) Height profile for the dashed lines given in corresponding AFM images.

The growth of MoS_2 thin films was also found dependent on the total pressure in the synthetic setup. Typically, higher pressures give rise to larger thickness. Figure S19 shows the optical images and Raman spectra of MoS_2 structures grown under widely different total pressures. The amount of $MoCl_5$ used in all these experiments was kept identical (15 mg). We can see that the MoS_2 thin film grown at a total pressure of 2 Torr shows bluish in color and has 2 layers with a Δk of 23.2 cm^{-1} in the Raman spectrum. In contrast, the thin film grown at 50 Torr is green and has a larger Δk of 25.3 cm^{-1} that is similar to that of bulk MoS_2 materials. This indicates a substantial larger thickness in the film grown at 50 Torr than the one grown at 2 Torr. An even larger total pressure can give rise to a growth of bulky structure such as triangular plates (Fig. S19d). The thickness of the triangular plates is measured as ~100-200 nm. Figure S20 gives another example to illustrate the effect of the total pressure on the growth. In these experiments, the amount of $MoCl_5$ used in these experiments was 4 mg, and we used different total pressures but kept all other conditions comparable. We can find that the Δk of the resulting thin film increases from 20.4 cm^{-1} at 2 Torr to 23.2 cm^{-1} at 10 Torr and further 24.6 cm^{-1} at 50 Torr. Again, this indicates that the layer number of the MoS_2 thin film increases with the total pressure.

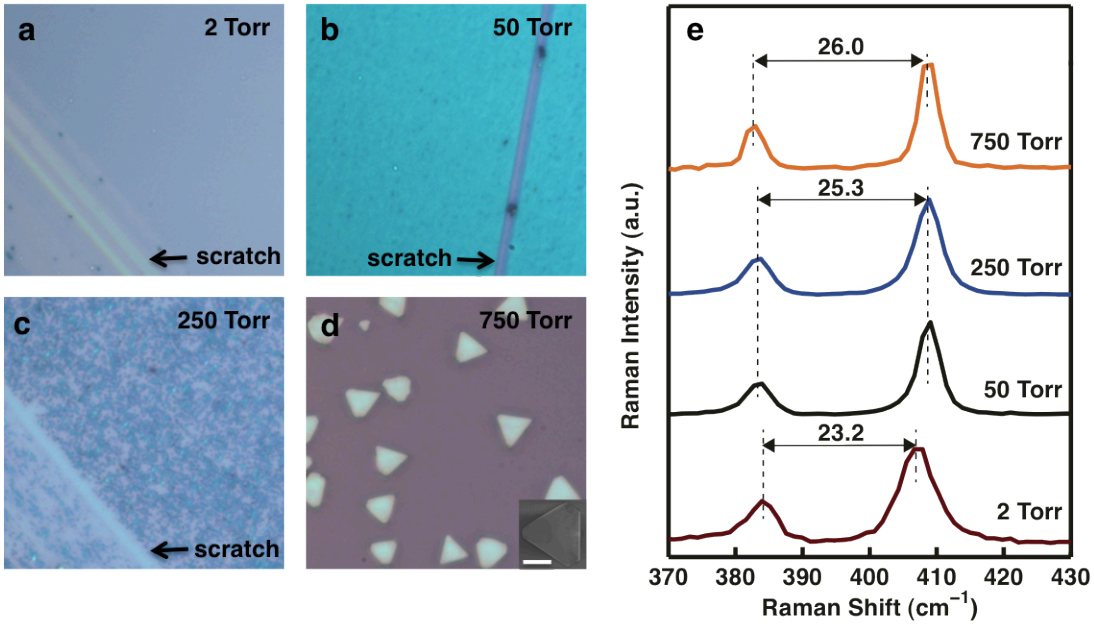

Fig. S19. MoS_2 materials grown under widely different total pressures. The amount of $MoCl_5$ used in these experiments is 15 mg. (a-d) Optical images of the MoS_2 materials grown with widely different total pressures, 2 Torr, 50 Torr, 250 Torr, and 750 Torr. Scratches were introduced to show the contrast between the film and the substrate (SiO_2/Si). (e) Raman spectra of the MoS_2 thin films grown under different total pressures. The total pressure for each of the Raman spectrum is labeled as shown. The Δk between the E^1_{2g} and A_{1g} peaks in the Raman spectra is also given in the figure.

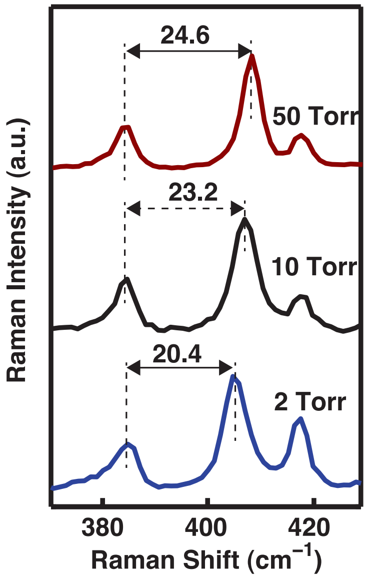

Fig. S20. Raman spectra of the MoS_2 thin films grown under different total pressures. The amount of $MoCl_5$ used in these experiments is 4 mg. And the total pressure for each of the Raman spectrum is labeled as shown. The Δk for the Raman spectra is also given in the figure. We can see that the thickness of the resulting thin film increases with the total pressure.

The effects of the amount of $MoCl_5$ precursor and the total pressure on the layer number of the synthesized MoS_2 thin film can be essentially correlated to their effects on the partial pressure of gaseous MoS_2 species. To illustrate this notion, we examined the synthetic process (Fig. S21). The synthetic process includes five major steps, 1) sublimation of sulfur and $MoCl_5$, 2) reaction of $MoCl_5$ and S to produce gaseous MoS_2 species, 3) transfer of the MoS_2 species downstream by carrier gas, 4) diffusion of MoS_2 species from the gas phase onto receiving substrates, 5) precipitation of MoS_2 on the substrates. In typical experiments, we use excessive amount of sulfur (the molar ratio of sulfur and $MoCl_5$ is > 1000:1) to ensure the vapor of S far bigger than that of $MoCl_5$. As a result, we can reasonably assume that the reaction of $MoCl_5$ is complete.

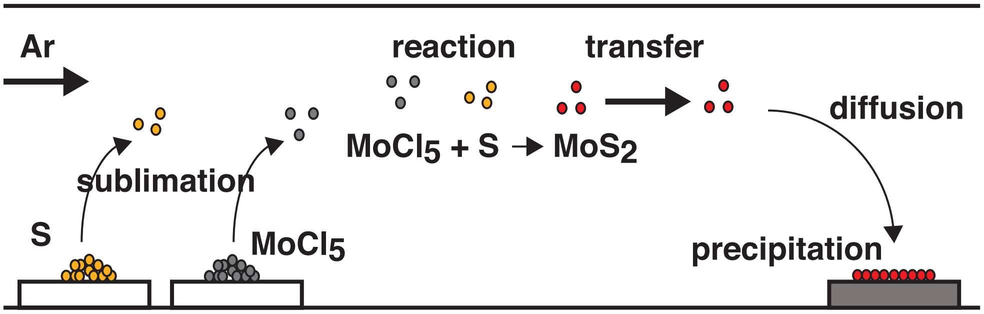

Fig. S21. Schematic illustration of the synthetic process, which includes five major steps: sublimation, reaction, transfer, diffusion, and precipitation.

With the assumption of the full reaction of $MoCl_5$ vapor, the partial pressure of MoS_2, P_{Mo}, depends on the sublimation rate (molar loss rate per unit surface area) of sulfur Φ_S and $MoCl_5$, Φ_{Mo}, the flow rate of carrier gas Ar, J_{Ar} (mol/s), and the total pressure P_{total} in the synthetic setup as

$$P_{Mo} = \frac{\Phi_{Mo} A_{Mo}}{\Phi_{Mo} A_{Mo} + \Phi_S A_S + J_{Ar}} P_{total} \qquad \text{(S1)}$$

A_{Mo} and A_S are the surface area of the precursor materials $MoCl_5$ and sulfur, respectively, which increases with the amount of precursor powder. The sublimation rate depends on the T of the precursor materials, and the difference between the equilibrium vapor pressure P_{vap} of precursor materials and the partial pressure P_{par} of these materials in vapor, $\Phi = (P_{vap} - P_{par}) / (2\pi MRT)^{0.5}$, where M is the molecular weight of the materials, and R is the molar gas constant. With the typical conditions used in experiments (the temperature at sulfur source is estimated T ~ 300°C, the weight of sulfur: 1g, the particle size in sulfur par: 0.1 mm), we can estimate that the sublimation flux of sulfur powder is around 0.015 mol/s. This is much larger than the typical flux (50 sccm) of carrier gas, $J_{Ar} \sim 0.0001$ mol/s. By the same token, we can also conclude that the sublimation flux of sulfur is orders of magnitude larger than that of $MoCl_5$. Therefore, during the synthesis period, eq. (S1) can be further simplified as

$$P_{Mo} = \frac{\Phi_{Mo} A_{Mo}}{\Phi_S A_S} P_{total} \qquad \text{(S2)}$$

From eq. (S2), we can see that the partial pressure of MoS_2 (P_{Mo}) increases with the amount of $MoCl_5$ precursor (increasing A_{Mo}) and the total pressure P_{total}. This correlation of the amount of $MoCl_5$ precursor and the total pressure with the partial pressure P_{Mo} strongly suggest that the partial pressure of MoS_2 species plays a key role in determining the layer number of the synthesized MoS_2 thin film. A larger partial pressure of gaseous MoS_2 species may give rise to MoS_2 films with larger layer numbers.

As corroborating evidence for our analysis, we observed that the flow rate of carrier gas bears negligible effects on the layer number of the MoS_2 films. Fig. S22 shows the Raman spectra collected from the MoS_2 thin films grown with different flow rates of carrier gas (Ar). We can find that the layer number of the thin films remains unchanged regardless a dramatic variation in the flow rate by one order of magnitude. This confirms the dominance of the sublimation flux of sulfur, which makes the flow rate of carrier gas only negligibly affect the partial pressure of MoS_2 species. This observation also confirms that the partial pressure of MoS_2 is indeed a key parameter to determine the layer number.

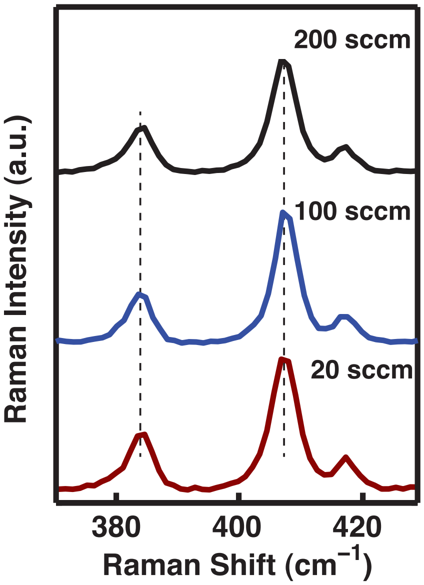

Fig. S22. Raman spectra of the MoS2 thin films grown under different flow rates of carrier gas. The total pressure was maintained to be 5 Torr. The two dashed lines indicates that the positions of E_{2g} and A_{1g} peaks remain identical regardless the flow rate.

To better elucidate the role of the partial pressure P_{Mo} in the control of the layer number, we further examine the dynamics of the synthetic process. Among all the five steps involved, of the most important for the growth is the rate-determining step. Typical rate-determining steps in chemical vapor deposition processes can be the diffusion or the precipitation, which is referred as diffusion-controlled or reaction-controlled, respectively. Our experimental results indicate that the growth of MoS_2 is reaction-controlled, i.e. the precipitation is the rate-determining step. This is supported by less deposition at lower pressure or higher temperature. We would expect the opposite, for instance, more deposition at lower pressures, should the rate-determining step is the diffusion step. Therefore, to understand the dependence of the layer number on the partial pressure of MoS_2, we examine the precipitation reaction,

$$MoS_2(g) \rightarrow MoS_2(s)$$

where *g* and *s* refer to gaseous and solid phases, respectively. This precipitation reaction is governed by two pressures, the partial pressure of gaseous species P_{Mo} and the equilibrium vapor pressure (referred as vapor pressure) of MoS_2 in solid phase (P^{o}_{Mo}). The role of P_{Mo} in control of the layer number is essentially rooted in its role in the thermodynamics and kinetics of the precipitation reaction. The difference between the partial pressure P_{Mo} and the vapor pressure $P^{\mathrm{o}}_{\mathrm{Mo}}$ provides the thermodynamic driving force for the precipitation reaction. The partial pressure must be larger than the vapor pressure, i.e., $P_{\mathrm{Mo}} > P^{\mathrm{o}}_{\mathrm{Mo}}$, to drive the precipitation of gaseous MoS_2 species. Additionally, based on the law of mass reaction, we know that the partial pressure P_{Mo} also dictates the rate of the precipitation, a larger P_{Mo} driving a faster precipitation.

The observed dependence of the layer number of MoS_2 films on experimental parameters (the amount of precursor materials and the total pressure) suggests that a larger partial pressure P_{Mo} tends to give rise to a thicker film (Fig. S21-S22). While a larger P_{Mo} can cause a larger precipitation rate, we do not think that this kinetic effect would be the major reason for the observed control of layer number. Should the precipitation rate be the major mechanism for the control, it would request a perfect control in timing to stop the precipitation right at the end of the formation of each individual layer, in order to produce the observed uniform MoS_2 films with precisely controlled layer number. This is most unlikely in our synthetic setup. The growth of large-area, highly uniform MoS_2 thin films in our experiments suggests that this precipitation is a self-limiting process, i.e. the precipitation automatically stops at the end of the formation of each individual layer.

We believe that the self-limiting mechanism may lie in a thermodynamic balance between the partial pressure of gaseous MoS_2 species P_{Mo} and the vapor pressure of MoS_2 thin films ($P^{\mathrm{o}}_{\mathrm{Mo}}$) on the substrate. The vapor pressure of MoS_2 thin films could depend on, more specifically, increase with the layer number. As P_{Mo} is requested larger than $P^{\mathrm{o}}_{\mathrm{Mo}}$ to provide the thermodynamic driving force, the precipitation of gaseous MoS_2 species may be automatically stopped at a specific layer number by control of P_{Mo}. For instance, an exclusive growth of MoS_2 monolayer could be achieved by controlling the partial pressure P_{Mo} between the vapor pressures of MoS_2 monolayer ($P^{\mathrm{o}}_{\mathrm{Mo},1}$) and bilayer ($P^{\mathrm{o}}_{\mathrm{Mo},2}$) films as $P^{\mathrm{o}}_{\mathrm{Mo},1} < P_{\mathrm{Mo}} < P^{\mathrm{o}}_{\mathrm{Mo},2}$. In this case, the larger vapor pressure of MoS_2 bilayers may automatically prevent the continuous growth once a MoS_2 monolayer film is formed, regardless a continuous supply of MoS_2 species. This indeed matches our observations that the lay number of MoS_2 films shows a step-function dependence on the amount of precursor materials (Table S1). Our hypothesis on the self-liming mechanism can also be supported by the observed dependence of the layer number on growth temperatures. We find that the layer number of MoS_2 film increases with the temperature of receiving substrates decreasing (Fig. S23). As illustrated in the Fig. S23 inset, we placed two receiving substrates in the synthetic setup, and examined the layer number of the MoS_2 thin film grown on these substrates. These substrates had different local temperatures, 850 °C, and 650 °C for the substrate 1 (referred as sub1 in Fig.S23 inset), and substrate 2, respectively. We can find that the layer number of the thin film increases with the temperature of receiving substrates decreasing. This can be understood that the vapor pressure of MoS_2 thin films $P^{\mathrm{o}}_{\mathrm{Mo}}$ decreases with the temperature, and the same partial pressure P_{Mo} can drive a deposition of thicker films at lower temperatures.

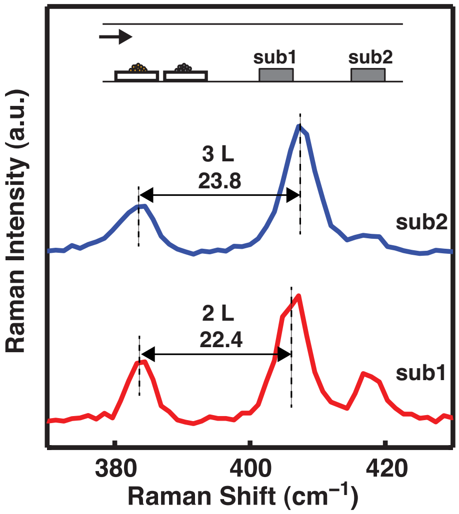

Fig. S23. Raman spectra of the MoS_2 thin films grown on receiving substrates with different temperatures. The inset shows a schematic illustrate of the experimental configuration. The temperature for the substrates can be estimated as 850°C (sub1) and 650°C (sub2).The layer number and the Δk in the Raman spectra of the films grown on these substrates are given as shown.

The dependence of the vapor pressure of MoS_2 thin films on the layer number might be related with the interaction with substrates. The vapor pressure indicates a capability of atoms escaping from solid phase into gas phase. The interaction of MoS_2 overlayers with substrates could substantially suppress the escaping of MoS_2 atoms, and subsequently cause a decrease in the vapor pressure. This interaction with substrates is expected to relax with the layer number (Fig. S24). As a result, the vapor pressure of MoS_2 thin film may increase with the layer number. Similar suppression effects of substrates on the vapor pressure have been well demonstrated in other materials adsorbed on substrates, for instance, polymers. [1] This dependence of vapor pressures on the layer number of MoS_2 films may provide the possibility of self-limiting growth. We also find in experiments that a precise control of the layer number generally tends to be more difficult for thicker films, for instance, larger than 4, often resulting a mixture of layer numbers. This suggests that the difference between the vapor pressures of MoS_2 films with neighboring layer number ($P^o_{Mo,n+1}$ - $P^o_{Mo,n,}$ n refers to the layer number) tends to shrink with an increase in the layer number, which makes the selective growth more difficult.

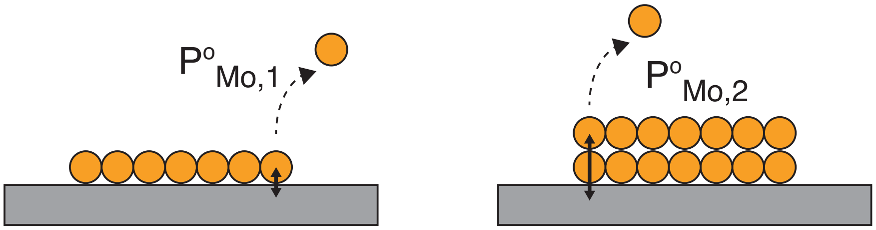

Fig. S24. Schematic illustration of the interaction between MoS_2 overlayers and receiving substrates. The vertical arrows indicate the interaction of the overlayer with the substrate. And the dashed line indicates the escaping of atoms from the solid phase into the gas phase.

To further examine the role of the interaction with substrates, we studied the growth on different receiving substrates, the traditional three-dimensional (3D) bonded materials such as sapphire (referred as 3D substrates) and highly ordered pyrolytic graphite (HOPG, from Ted Pella) that has a similar layered structure as MoS_2 (referred as 2D substrates). We grew MoS_2 films on these different substrates under identical experimental conditions (the different substrates were placed side by side in the tube furnace). We can find a substantial difference between the films grown on sapphire and HOPG (Fig. S25). With the same experimental conditions, while the film grown on sapphire substrates is monolayer (Δk 20.4 cm^{-1}), the one grown on HOPG is bilayer (Δk 22.4 cm^{-1}). We can exclude out that the observed difference in the Raman shifts is caused by the difference in substrates. As a control experiment, we transferred the monolayer MoS_2 grown on sapphire to HOPG substrates, and measured the Raman scattering from the transferred monolayer MoS_2. We can find that the Raman peak of the transferred MoS_2 is identical to the as-grown MoS_2 monolayer on sapphire substrates.

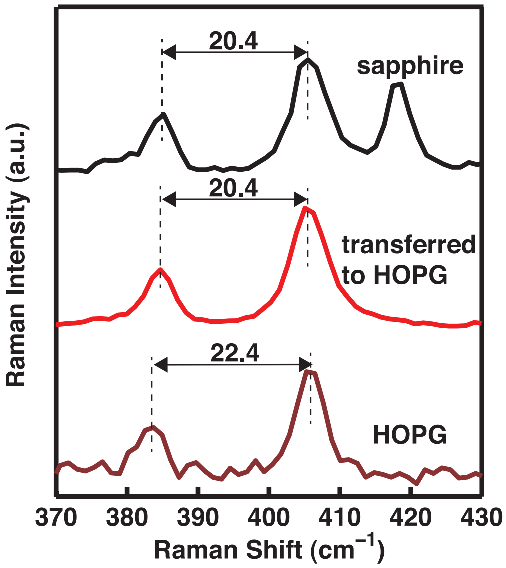

Fig. S25. Raman spectra of the MoS_2 thin films grown on different substrates. These substrates were placed side by side in the same experiments. All the experimental conditions for the growth on these substrates were kept identical. The layer number and the Δk in the Raman spectra of the films grown on these substrates are given as shown.

This result confirms that the interaction of MoS_2 films with substrates plays an important role in the self-limiting growth. The strength of the interaction of 2D material overlayer with conventional 3D substrates e.g. sapphire, is well known different from that with 2D substrates (such as HOPG). This difference has been extensively manifested by the van del Waals epitaxial growth of layered materials on 2D substrates.[2] In our experiment, the different interactions of MoS_2 films with sapphire and HOPG might cause different vapor pressures. Therefore, the same partial pressure of MoS_2 can give rise to a growth of thicker MoS_2 film on HOPG.

References

1 Podgornik, P. & Parsegian, V. A. On a possible microscopic mechansm underlying the vapor pressure paradox. *Biophy. J.* **72**, 942-952, (1997).

2 Ueno, K., Saiki, K., Shimada, T. & Koma, A. Epitaxial growth of transition metal dichalcogenides on cleaved faces of mica. *J. Vac. Sci. Technol. A* **8**, 68, (1990).